Biochemical and Biophysical Research Communications 499 (2018) 862–867

Contents lists available at ScienceDirect

Biochemical and Biophysical Research Communications

journal homepage: www.elsevier.com/locate/ybbrc

Structural requirement of the hydrophobic region of the *Bordetella pertussis* CyaA-hemolysin for functional association with CyaC-acyltransferase in toxin acylation

Veerada Raksanoh [a, b, 1], Panchika Prangkio [b, 1], Chompounoot Imtong [c], Niramon Thamwiriyasati [d], Kittipong Suvarnapunya [e, f], Lalida Shank [b, *], Chanan Angsuthanasombat [f, g, **]

[a] Interdisciplinary Program in Biotechnology, Graduate School, Chiang Mai University, Chiang Mai 50200, Thailand
[b] Division of Biochemistry and Biochemical Technology, Department of Chemistry, Center of Excellence in Bioresources for Agriculture, Industry and Medicine, Center of Innovation in Chemistry (PERCH-CIC), Faculty of Science, Chiang Mai University, Chiang Mai 50200, Thailand
[c] Division of Biology, Department of Science, Faculty of Science and Technology, Prince of Songkla University, Pattani 94000, Thailand
[d] Department of Medical Technology, Faculty of Allied Health Sciences, Burapha University, Chonburi 20131, Thailand
[e] Graduate Program in Immunology, Faculty of Medicine Siriraj Hospital, Mahidol University, Bangkok 10700, Thailand
[f] Bacterial Toxin Research Innovation Cluster (BRIC), Institute of Molecular Biosciences, Mahidol University, Salaya Campus, Nakornpathom 73170, Thailand
[g] Laboratory of Molecular Biophysics and Chemical Biology, Biophysics Institute for Research and Development (BIRD), Fang, Chiang Mai 50110, Thailand

ARTICLE INFO

Article history:
Received 26 March 2018
Accepted 1 April 2018
Available online 7 April 2018

Keywords:
CyaA-RTX
CyaC-acyltransferase
Electrostatic potentials
Hydrophobic region
Palmitoylation
Protein association

ABSTRACT

Previously, we demonstrated that the ~130-kDa CyaA-hemolysin (CyaA-Hly, Met^{482}-Arg^{1706}) from *Bordetella pertussis* was palmitoylated at Lys^{983} when co-expressed with CyaC-acyltransferase in *Escherichia coli*, and thus activated its hemolytic activity. Here, further investigation on a possible requirement of the N-terminal hydrophobic region (HP, Met^{482}-Leu^{750}) for toxin acylation was performed. The ~100-kDa RTX (Repeat-in-ToXin) fragment (CyaA-RTX, Ala^{751}-Arg^{1706}) containing the Lys^{983}-acylation region (AR, Ala^{751}-Gln^{1000}), but lacking HP, was co-produced with CyaC in *E. coli*. Hemolysis assay indicated that CyaA-RTX showed no hemolytic activity. Additionally, MALDI-TOF/MS and LC-MS/MS analyses confirmed that CyaA-RTX was non-acylated, although the co-expressed CyaC-acyltransferase was able to hydrolyze its chromogenic substrate–*p*-nitrophenyl palmitate and acylate CyaA-Hly to become hemolytically active. Unlike CyaA-RTX, the ~70-kDa His-tagged CyaA-HP/BI fragment which is hemolytically inactive and contains both HP and AR was constantly co-eluted with CyaC during IMAC-purification as the presence of CyaC was verified by Western blotting. Such potential interactions between the two proteins were also revealed by semi-native PAGE. Moreover, structural analysis *via* electrostatic potential calculations and molecular docking suggested that CyaA-HP comprising α1-α5 (Leu^{500}-Val^{698}) can interact with CyaC through several hydrogen and ionic bonds formed between their opposite electrostatic surfaces. Overall, our results demonstrated that the HP region of CyaA-Hly is conceivably required for not only membrane-pore formation but also functional association with CyaC-acyltransferase, and hence effective palmitoylation at Lys^{983}.

1. Introduction

Adenylate cyclase-hemolysin toxin (CyaA) is a major virulence factor secreted from *Bordetella pertussis*, a Gram-negative pathogen that causes whooping cough (also known as 'pertussis') in humans, a serious respiratory infectious disease [1]. CyaA, which belongs to the class of RTX (Repeat-in-ToXin) cytolysins, is able to facilitate respiratory tract colonization of *B. pertussis* by impairing defense function of host macrophages [2]. Whooping cough has now re-

Abbreviations: AR, acylation region; CyaA, adenylate cyclase-hemolysin toxin; IMAC, immobilized-metal ion affinity chromatography; HP, hydrophobic region; pNPP, *p*-nitrophenyl palmitate; RTX, Repeat-in-ToXin.

* Corresponding author.
** Corresponding author. Bacterial Toxin Research Innovation Cluster (BRIC), Institute of Molecular Biosciences, Mahidol University, Salaya Campus, Nakornpathom 73170, Thailand.
E-mail addresses: lalida.shank@cmu.ac.th (L. Shank), chanan.ang@mahidol.ac.th (C. Angsuthanasombat).
[1] Authors with equal contributions.

https://doi.org/10.1016/j.bbrc.2018.04.007
0006-291X/

emerged worldwide as a consequence of declining immunity, following vaccination and imperfect vaccination of populations [3], hence requiring novel approaches for treatment. Recently, we have successfully generated CyaA-specific humanized VH/V_HH nanobodies that would have potential applications in developing a novel anti-pertussis agent [4].

Unlike other RTX cytolysins, the 1706-residue CyaA toxin (~180-kDa) consists of two functionally different domains: the ~40-kDa N-terminal adenylate cyclase (AC) and the ~130-kDa C-terminal pore-forming or hemolysin (Hly) domains [5] (*see* Supplementary Fig. 1). While translocation of the AC domain into the target cell interior is known to induce an increase in pathological levels of cAMP, resulting in apoptosis [6], multiple sources of evidence revealed that the Hly domain is responsible for hemolysis against sheep erythrocytes and ion-channel formation in planar lipid bilayers [7,8]. Of particular interest in the Hly domain (residues ~400–1700), there are four important regions, including (*i*) a pore-forming hydrophobic region (HP, residues ~400–750) containing transmembrane helices of which α2 and α3 are likely to participate in membrane-pore formation [9–12], (*ii*) an acylation region (AR, residues ~750–1000) with the Lys^{983}-acylation site [13,14], (*iii*) a receptor-binding RTX region (residues ~1000–1700) containing Gly-Asp nonapeptide repeats that serve as Ca^{2+}-binding sites [15,16] and (*iv*) a secretion signal [17]. The binding of Ca^{2+} ions has been independently demonstrated to play a key role in providing either structural stability against proteolytic degradation [18] or proper folding into a β-roll structure of the CyaA-RTX region [19].

CyaA is initially produced as an inactive pre-protoxin of ~180 kDa and after removal of the signal sequence, it becomes activated by a post-translational palmitoylation of Lys^{983} mediated by the endogenous CyaC-acyltransferase [13]. According to functional requirements of lipid acylation at Lys^{983} for both cytotoxic and hemolytic activities [7,20], the Lys^{983}-linked palmitoyl moiety was proposed to enhance membrane association of the full-length CyaA toxin *via* receptor binding [21]. However, our recent studies showed that such toxin modification *via* Lys^{983}-palmitoylation was not required for binding of the 130-kDa CyaA-Hly domain to target erythrocyte membranes, but it appeared to be involved in stabilizing toxin-induced ion-leakage pores [22].

Previously, we demonstrated that a ~100-kDa truncated fragment of CyaA-Hly (*i.e.*, CyaA-RTX, Ala^{751}-Arg^{1706}), recombinantly produced without an acylation-mediating CyaC, could still bind to sheep erythrocyte membranes, although it showed no hemolytic activity [23]. However, there was no direct evidence to support whether the lack of HP region (Met^{482}-Leu^{750}) at the N-terminus of the CyaA-RTX truncate would indeed lead to the disappearance of toxin acylation, hence limiting its hemolytic activity. In this study, this truncated CyaA-RTX fragment with the Lys^{983}-acylation region (Ala^{751}-Gln^{1000}) was therefore co-produced with CyaC-acyltransferase in order to determine if the HP region would contribute to toxin acylation. Our results suggested a potential requirement of such HP region for specific binding of CyaC prior to its effective acylation. Additionally, an apparent association during protein purification was observed between CyaC and a smaller CyaA-Hly truncate, *i.e.*, 70-kDa CyaA-HP/BI which is hemolytically inactive and consists of HP, AR and the first block of the RTX region (*see* Supplementary Fig. 1). Moreover, structural analysis *via* molecular docking revealed several hydrogen bonding and ionic interactions formed between CyaC-acyltransferase and the ~20-kDa CyaA-HP segment comprising α1-α5 (Leu^{500}-Val^{698}), as supporting evidence of their potential association for toxin acylation.

2. Materials & methods

2.1. Construction of recombinant plasmid

pCyaAC-PF plasmid encoding both ~130-kDa CyaA-Hly and ~22-kDa CyaC-acyltransferase under control of the T_7 promoter [7] was used as a template for gene manipulation. Construction of pCyaAC-RTX plasmid co-expressing CyaA-RTX (Ala^{751}-Arg^{1706}) and CyaC was accomplished by deletion of the gene segment encoding the ~30-kDa N-terminal HP region (*i.e.*, Met^{482}-Leu^{750}) from the original pCyaAC-PF to which an additional *Nde*I site was introduced by site-directed mutagenesis. The 6747-bp *Nde*I-digested DNA fragment corresponding to pCyaAC-RTX was gel-purified and re-ligated. The resulting plasmid was transformed into *E. coli* strain BL21(DE3)pLysS and verified by DNA sequencing.

2.2. Expression and preparation of CyaA-RTX

E. coli cells strain BL21(DE3)pLysS harboring the pCyaAC-RTX plasmid were grown at 30 °C in Luria-Bertani medium containing 100 μg/mL ampicillin until OD_{600} of the culture reached 0.5–0.6. After addition of isopropyl-β-D-thiogalactopyranoside (IPTG) to a final concentration of 0.1 mM, incubation was continued under the same condition for another 6 h. The IPTG-induced *E. coli* samples were analyzed for protein expression level by sodium dodecyl sulfate-(12% w/v) polyacrylamide gel electrophoresis (SDS-PAGE).

After centrifugation, *E. coli* cells expressing CyaA-RTX together with CyaC were washed twice with hemolysis buffer (5 mM $CaCl_2$, 125 mM NaCl, 20 mM HEPES, pH 7.4). The washed cell pellets were re-suspended in the buffer containing 1 mM phenylmethylsulfonyl fluoride and subsequently disrupted using an ultrasonic processor. The resulting cell lysate was centrifuged (8000×*g*, 4 °C, 15 min) and the supernatant, referred as crude lysate, was then carefully transferred to a new tube. Concentrations of total proteins (including CyaA-RTX) in the crude lysate were determined by Bradford-based microassay.

2.3. Expression and purification of CyaA-HP/BI

The ~70-kDa His-tagged CyaA-HP/BI protein was expressed and subsequently purified as described previously [24]. Briefly, after 6-h IPTG-induction, cell pellets were harvested and incubated with lysozyme at 4 °C overnight followed by ultrasonication. Inclusion bodies were separated by centrifugation (8000×*g*, 4 °C, 15 min) and subsequently denatured with 4 M urea. His-tagged soluble protein samples were purified by immobilized-metal ion affinity chromatography (IMAC) using a Ni^{2+}-NTA (nickel-nitrilotriacetic acid) column and subsequently desalted through a PD10 column.

2.4. Hemolytic activity assay

In vitro hemolytic activity of the tested samples against sheep red blood cells (sRBC) was assessed as described previously [7], with some modifications. Soluble *E. coli* lysate expressing CyaA proteins (CyaA-RTX or CyaA-Hly) was diluted to desired concentrations and the volume was adjusted to 980 μL with hemolysis buffer before addition of 20-μL sRBC (~10^8 cells). The sample-sRBC mixtures were incubated at 37 °C for 5 h. Unlysed erythrocytes were removed by centrifugation (12,000 × *g*, 2 min) and released hemoglobin in the supernatant was measured at OD_{540}. Crude lysate containing pET17b was used as a negative control. OD_{540} value corresponding to complete hemolysis was obtained by lysing

sRBC with 0.1% Triton-X 100. Percentage of hemolysis caused by individual tested samples was calculated by {[OD_{540} sample − OD_{540} negative control]/[OD_{540} of complete hemolysis − OD_{540} negative control]} × 100. All samples were assessed in triplicates for each experiment.

2.5. Mass spectrometric analyses

Target protein bands resolved by SDS-PAGE were individually excised and eluted from the gel prior to digestion with trypsin according to a standard protocol. Two approaches, MALDI-TOF/MS (matrix-assisted laser desorption ionization-time of flight mass spectrometry, Bruker Reflex IV MALDI-TOF Mass Spectrometer) and LC-MS/MS (liquid chromatography-tandem mass spectrometry, Thermo Finnigan LTQ Ion Trap Mass Spectrometer), were used to analyze the purified trypsin-generated peptide fragments.

2.6. Ester-bond hydrolysis assay

Purified soluble CyaC from *E. coli* cells harboring pCyaAC-RTX was prepared by three consecutive chromatographic techniques as described previously [25] and assessed for its esterase activity in comparison with that from pCyaAC-PF. *p*-nitrophenyl palmitate (pNPP) was used as a chromogenic substrate. Purified CyaC (~4.5 μg) was mixed with 300 μL of 50 mM Tris-HCl (pH 7.4) containing 100 μM pNPP. Esterase activity was then determined by detecting the formation of *p*-nitrophenol product using spectrophotometer at OD_{400}.

2.7. Western blot analysis

To determine the presence of CyaC-acyltransferase, the protein samples of interest were subjected to SDS-PAGE and transferred onto a nitrocellulose membrane. After blocking with 5% skim milk in PBS (phosphate buffer saline, pH 7.4), the membrane was serially probed with mouse anti-CyaC antiserum (1:5000 dilution) and alkaline phosphatase (ALP)-conjugated goat anti-mouse IgGs (1:7000 dilution). Color detection was done by incubation with 5-bromo-4-chloro-3-indolyl phosphate/nitroblue tetrazolium substrates.

2.8. Protein association assay

The co-eluted protein fraction from the affinity-based Ni^{2+}-NTA column, containing both CyaA-HP/BI and CyaC proteins was assessed for their association on a semi-native PAGE system containing SDS only in gel and running buffers [26]. Protein samples were prepared in loading dye buffer with or without (semi-native) 2% SDS, 25 mM DTT and boiling prior to analysis on SDS-PAGE with regular 0.1% SDS.

2.9. Homology-based modeling

A plausible 3D-model of CyaC was generated based on the crystal structure of the toxin-activating acyltransferase from *Actinobacillus pleuropneumoniae* (PDB ID: 4WHN) [27] while that of CyaA-HP comprising α1-α5 (Leu^{500}-Val^{698}) [28] was built based on the best-fit template structure of bovine rhodopsin (PDB ID: 1GZM) [29] by using SWISS-MODEL homology-based modeling. Both models were constructed according to the target-template alignment using ProMod3 [30]. A force field was used for regularization of the resulting model's geometry. Quality of global and per-residue models was assessed using the QMEAN scoring function [31].

2.10. Calculations of electrostatic potentials

Poisson-Boltzmann electrostatic calculations on both refined 3D models of CyaC and CyaA-HP were performed using the Adaptive Poisson-Boltzmann Solver (APBS) [32] with AMBER force field. The calculations were performed with pH of 7.4.

2.11. Molecular docking

Protein-protein docking between CyaC and CyaA-HP modeled structures was performed using ClusPro 2.0 automated docking server [33]. The resulting docking complex was analyzed by using PyMOL program.

3. Results and discussion

3.1. Functional and biochemical characteristics of CyaA-RTX co-expressed with CyaC-acyltransferase

Recently, we have demonstrated that the requirement of acylation by CyaC-acyltransferase for CyaA-Hly-induced hemolytic activity is not directly implicated in toxin binding to target erythrocyte membranes, but rather involved in efficient membrane-pore formation [22]. In agreement with such findings, we also found that the CyaA-RTX truncate (Ala^{751}-Arg^{1706}) produced without CyaC could competitively block the binding of CyaA-Hly to sRBC membranes, although it exerted no hemolytic activity [23]. In the present study, we therefore further investigated to see whether a defect in the toxin-induced hemolytic activity observed with CyaA-RTX, albeit containing the Lys^{983}-acylation region (Ala^{751}-Gln^{1000}) (*see* Supplementary Fig. 1), is related to the deficiency in toxin acylation or the disappearance of the membrane-inserting HP region (Met^{482}-Leu^{750}). Herein, another recombinant plasmid, *i.e.*, pCyaAC-RTX, encoding both the CyaA-RTX truncate and CyaC-acyltransferase, was initially constructed. Upon IPTG-induction, *E. coli* cells harboring pCyaAC-RTX were found to produce ~100-kDa CyaA-RTX as well as ~22-kDa CyaC in both soluble and inclusion forms (Fig. 1, *right panel*), consistent with our previous observation when the CyaA-RTX fragment was produced without CyaC [23]. When the crude lysate containing the soluble CyaA-RTX fragment together with CyaC was assessed for its lytic activity against sRBC, significant hemolysis was barely observed (~3%) as compared with that bearing the acylated CyaA-Hly (~40%) (*see* Fig. 2). These results indicate that the lack of HP region at the N-terminus of the CyaA-RTX truncate would give rise to the non-hemolytic character regardless of co-expression with CyaC-

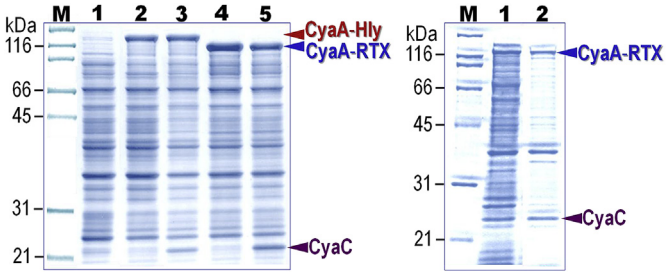

Fig. 1. *Left panel*, SDS-PAGE (Coomassie brilliant blue-stained 10% gel) analysis of lysates extracted from *E. coli* cells harboring pCyaA-PF (lane 2) pCyaAC-PF (lane 3), pCyaA-RTX (lane 4) and pCyaAC-RTX co-expressing CyaA-RTX and CyaC-acyltransferase (lane 5). Cells harboring the pET17b vector were used as a negative control (lane 1). *Right panel*, SDS-PAGE (Coomassie brilliant blue-stained 10% gel) analysis of soluble (lane 1) and insoluble (lane 2) fractions of *E. coli* cells harboring pCyaAC-RTX. M, molecular mass standards. (For interpretation of the references to color in this figure legend, the reader is referred to the Web version of this article.)

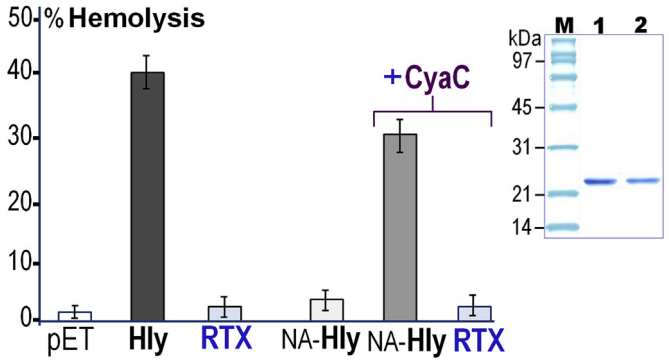

Fig. 2. Hemolytic activities against sRBC of lysate from *E. coli* cells (~10^8) containing ~5 μg of CyaA-Hly, CyaA-RTX co-expressed with CyaC-acyltransferase, or NA-CyaA-Hly (non-acylated CyaA-Hly) without CyaC. The crude cell lysate containing the pET-17b vector alone was used as a negative control. Error bars indicate standard errors of the mean from three independent experiments where each sample was performed in triplicate. *Inset*, SDS-PAGE (Coomassie brilliant blue-stained 12% gel) of CyaC purification. Lanes 1 and 2, ~22-kDa purified CyaC-acyltransferase from *E. coli* cells harboring pCyaAC-RTX and pCyaAC-PF, respectively. M, molecular mass standards. (For interpretation of the references to color in this figure legend, the reader is referred to the Web version of this article.)

acyltransferase.

Further attempts were made to determine whether the loss of hemolytic activity of CyaA-RTX co-expressed with CyaC could essentially result from the lack of HP region, not the defect in toxin acylation. CyaA-RTX was thus subjected to MALDI-TOF/MS and LC-MS/MS analyses for verifying the existence of palmitoyl ($C_{16:0}$) moiety at Lys^{983}. Unexpectedly, despite the presence of both CyaC-acyltransferase and the CyaC-targeting AR region on the CyaA-RTX fragment, no acylation was detected within the truncate. As can be illustrated, the trypsin-digested fragment encompassing Lys^{983} (E^{972}GVATQTAAYGK^{983}, m/z ratio = 1226.61) substantiated that the palmitoyl group at Lys^{983} is absent in CyaA-RTX when compared to its corresponding fragment derived from CyaA-Hly (E^{972}GVATQTAAYGK$_{16:0}$R^{984}, m/z ratio = 1619.75). These results clearly indicated that the lack of HP region at the N-terminus of CyaA-RTX would lead to the deficiency in toxin acylation by CyaC.

3.2. *In vitro verified activities of co-expressed CyaC via CyaA-Hly activation and substrate hydrolysis*

As mentioned earlier, the ~130-kDa CyaA-Hly domain, but not the ~100-kDa CyaA-RTX truncate, can be palmitoylated at Lys^{983} *in vivo* by the co-expressed CyaC-acyltransferase for activating its hemolytic activity. By this activation analogy, we have thus used this 130-kDa fragment as an acylated target for verifying the activating activity of the soluble CyaC which was co-expressed with the CyaA-RTX truncate (*see* Fig. 1, *right panel*, *lane 1*). When the cell lysate containing non-acylated CyaA-Hly (Fig. 1, *left panel*, *lane 2*) was mixed with CyaC, it showed high hemolytic activity against sRBC (~30%) whereas the lysate containing CyaA-RTX mixed with CyaC or non-acylated CyaA-Hly alone exhibited very low activity (≤5%) (*see* Fig. 2). These results verified that the purified co-expressed CyaC-acyltransferase was able to acylate the CyaA-Hly fragment *in vitro*, but not CyaA-RTX, and hence activating the CyaA-Hly-induced hemolytic activity. Thus, this hemolytic activity could be inferred as the verified capability of CyaC co-expressed with CyaA-RTX in transferring palmitoyl group to the suitable acceptor, CyaA-Hly.

Previously, we have developed a spectrophotometric assay for assessing the ester-bond hydrolytic activity of CyaC-acyltransferase *via* detection of its esterase activity using an indolyl substrate (*i.e.*, *p*-nitrophenyl palmitate, pNPP) containing a palmitoyl ($C_{16:0}$) unit [25]. Herein, when such established hydrolysis assay was performed, it was verified that the purified CyaC co-expressed with the ~100-kDa CyaA-RTX truncate could still function as efficiently as that co-expressed with the ~130-kDa CyaA-Hly fragment (*see* Supplementary Table 1). As can be also seen in Supplementary Table 1, specific activities of the CyaC-acyltransferase purified from both lysates (*see* Fig. 2, *inset*) in catalyzing pNPP are comparable (~250 U/mg) and consistent with the above results for the CyaA-Hly-induced hemolytic activity upon *in vitro* activation by CyaC which was co-expressed with CyaA-RTX (*see* Fig. 2). Taken together, these observations suggested that the N-terminal HP region, apart from the AR region encompassing Lys^{983}, is an additional part required for an appropriate docking of CyaC onto the CyaA-Hly molecule since the CyaA-RTX truncate, lacking only HP, as opposed to the hemolytically-active CyaA-Hly fragment, cannot be palmitoylated at Lys^{983} by the verified functional CyaC-acyltransferase.

3.3. *Potential association between CyaC-acyltransferase and HP-containing fragment*

As suggested above, the N-terminal HP region (Met^{482}-Leu^{750}) is conceivably required for a proper interaction of CyaA-Hly with CyaC-acyltransferase, and hence toxin acylation. This suggestion was supported by further experimental observation during on-column refolding in IMAC-purification that the ~70-kDa His-tagged CyaA-HP/BI truncate (*see* Supplementary Fig. 1) was always co-eluted with the non-His-tagged co-expressed CyaC which was verified by probing with anti-CyaC antiserum in Western blotting (Fig. 3). It should be noted that the two proteins, *i.e.* CyaA-HP/BI with Zn^{2+}-dependent autocatalytic activity [24] and CyaC-acyltransferase, were likely refolded into their native conformations as indicated by their recovery of enzymatic activities [24,25].

Further assessment to verify whether CyaC-acyltransferase and such a HP-comprising protein (*i.e.*, CyaA-HP/BI) are strongly associated was performed by utilizing modified SDS-PAGE, a semi-native PAGE system containing SDS only in gel and running buffers and no boiling of the samples [26]. The results as shown in Fig. 3 reveal that, with our experimental settings, the ~22-kDa co-eluted CyaC protein could apparently associate with the CyaA-HP/BI's autodegradation fragments on the gel under a semi-native

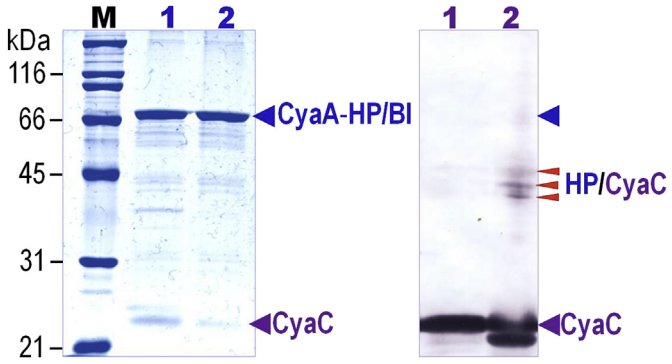

Fig. 3. *Left panel*, SDS-PAGE (Coomassie brilliant blue-stained 10% gel) analysis of protein samples containing the CyaA-HP/BI fragment and CyaC-acyltransferase co-eluted from Ni^{2+}-NTA affinity column prepared in loading dye buffer with (lane 1) or without (lane 2) 2% SDS, 25 mM 1,4-dithiothreitol and boiling. M, molecular mass standards. *Right panel*, Western blot analysis of the protein samples corresponding to those in the left panel-SDS-PAGE probed with anti-CyaC antibody. Besides the reactive band with the size of ~21-kDa CyaC-acyltransferase, several antibody-reactive bands of ~45–50 kDa are indicated by red arrows. (For interpretation of the references to color in this figure legend, the reader is referred to the Web version of this article.)

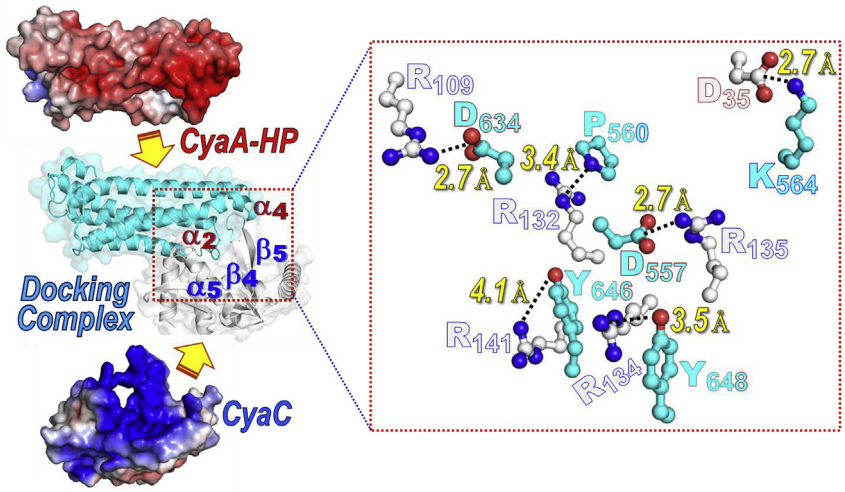

Fig. 4. Protein-protein interactions between CyaA-HP and its counterpart, CyaC-acyltransferase. Individual protein molecules of CyaA-HP comprising α1-α5 (*top*) and CyaC (*bottom*) are shown as surface representation colored according to the electrostatic potential values (negative, red; positive, blue). Docking complex of the protein counterparts (*middle*) is depicted as schematic ribbons with transparent surface representation and protein regions contributing high electrostatic potentials to the protein molecules are indicated. *Inset*, a zoom-in region showing potential interactions of CyaC-acyltransferase (white) and the CyaA-HP fragment (cyan) *via* hydrogen and ionic bonds (indicated as dotted lines). (For interpretation of the references to color in this figure legend, the reader is referred to the Web version of this article.)

condition. As can be seen that a few positive bands of CyaC-antibody reactive complexes of ~45–50 kDa were evidently detected (*see* Fig. 3, *right panel*, *lane 2*) while these reactive bands were not visualized under strongly denaturing conditions (Fig. 3, *right panel*, *lane 1*). These results could signify that the potential interaction between CyaA-HP/BI and CyaC observed during IMAC-purification was strong enough to maintain the two-fragment associated complex under the employed semi-native condition with 0.1% SDS in the gel and electrode buffer. Such complex formation could possibly be mediated by intermolecular non-covalent interactions, particularly multiple polar interactions including a network of hydrogen (H) bonds and ionic interactions.

3.4. Docking between CyaA-HP and CyaC models supportive of their functional association

Thus far, the lack of 3D crystal structure for both CyaC-acyltransferase and the CyaA toxin or its truncated fragments has hampered the experimental characterization of the CyaC/CyaA-HP-interacting region. To gain critical insights into the architecture of such molecular interaction between the CyaC and the CyaA-HP region, attempts were therefore made to construct a plausible 3D-modeled structure of CyaC and its counterpart fragment, CyaA-HP (Leu^{500}-Val^{698}), a representative of the HP-carrying protein. Ramachandran plots of both homology-based models revealed that over 95% of the side-chains are found to reside in their original most favored locations with additional allowed positional flexibility, indicating that both modeled structures could remain in sterically favorable main-chain conformations.

When the CyaC refined model was subsequently determined for its electrostatic potentials at pH 7.4, apparent positive potentials were revealed on the protein surface made up of α5, β4 and β5 (*see* Fig. 4, *bottom*). On the other hand, electrostatic potentials of the CyaA-HP model revealed mostly negative, especially strongly negative surface potentials at the C-terminal part of α2 and α4 (Fig. 4, *top*). Hence, it is conceivable that such attractive electrical forces *via* the opposite surface potentials between the two proteins would initially bring them close to each other, thus allowing other specific non-covalent interactions for further holding up their intermolecular association. Interestingly, when the CyaC model was docked with the CyaA-HP model, both models appeared to orientate themselves with respect to their opposite surface potentials (Fig. 4, *middle*). Further structural analysis of the docking complex revealed that the CyaC-acyltransferase model could specifically interact with the putative α2-α3 and α4-α5 loops on the CyaA-HP fragment through their several charged and polar residues (*i.e.*, Asp^{35}, Arg^{109}, Arg^{132}, Arg^{134}, Arg^{135} and Arg^{141} for CyaC; Asp^{557}, Lys^{564}, Asp^{634}, Tyr^{646} and Tyr^{648} for CyaA-HP), forming multiple H bonds and ionic interactions with bond length of 2.7–4.1 Å (Fig. 4, *inset*). These *in silico* data could validate that the CyaC-acyltransferase would specifically interact with the solvent-exposed loops within the CyaA-HP region, thus implicating a structural prerequisite of HP for CyaC in efficient acylation of CyaA-Hly. Taken as a whole, our present results provide evidence for the requirement of not only the Lys^{983}-acylation region (Ala^{751}-Gln^{1000}) but also the HP region (Met^{482}-Leu^{750}) encompassing transmembrane helices (α1-α5, Leu^{500}-Val^{698}) of the ~130-kDa CyaA-Hly pore-forming domain (Met^{482}-Arg^{1706}) for functional association with CyaC-acyltransferase, and hence effective toxin palmitoylation at Lys^{983}, signifying another important role of the CyaA-HP region in addition to toxin-induced pore formation.

Acknowledgement

This work was supported in part by grants from the Thailand Research Fund (MRG-56-8-0023, MRG-59-8-0040 and BRG-58-8-0002) as well as Mahidol University (MU 49/2559), and the Chiang Mai University Young Faculty Research Grant, Center of Excellence in Bioresources for Agriculture, Industry and Medicine, Faculty of Science, Chiang Mai University and PERCH-CIC. Thanks are also due to the reviewers for their constructive critiques.

Appendix A. Supplementary data

Supplementary data related to this article can be found at https://doi.org/10.1016/j.bbrc.2018.04.007.

Transparency document

Transparency document related to this article can be found

online at https://doi.org/10.1016/j.bbrc.2018.04.007.

References

[1] G. Fedele, M. Bianco, C.M. Ausiello, The virulence factors of *Bordetella pertussis*: talented modulators of host immune response, Arch. Immunol. Ther. Exp. 61 (2013) 445–457.

[2] J. Vojtova, J. Kamanova, P. Sebo, *Bordetella* adenylate cyclase toxin: a swift saboteur of host defense, Curr. Opin. Microbiol. 9 (2006) 69–75.

[3] E. Chiappini, A. Stival, L. Galli, M. de Martino, Pertussis re-emergence in the post-vaccination era, BMC Infect. Dis. 13 (2013) 151–162.

[4] A. Malik, C. Imtong, N. Sookrung, G. Katzenmeier, W. Chaicumpa, C. Angsuthanasombat, Structural characterization of humanized nanobodies with neutralizing activity against the *Bordetella pertussis* CyaA-hemolysin: implications for a potential epitope of toxin-protective antigen, Toxins 8 (2016) 99–111.

[5] R. Benz, E. Maier, D. Ladant, A. Ullmann, P. Sebo, Adenylate cyclase toxin (CyaA) of *Bordetella pertussis;* Evidence for the formation of small ion-permeable channels and comparison with HlyA of *Escherichia coli*, J. Biol. Chem. 269 (1994) 27231–27239.

[6] P. Gueirard, A. Druilhe, M. Pretolani, N. Guiso, Role of adenylate cyclase-hemolysin in alveolar macrophage apoptosis during *Bordetella pertussis* infection *in vivo*, Infect. Immun. 66 (1998) 1718–1725.

[7] B. Powthongchin, C. Angsuthanasombat, High level of soluble expression in *Escherichia coli* and characterisation of the CyaA pore-forming fragment from a *Bordetella pertussis* Thai clinical isolate, Arch. Microbiol. 189 (2008) 169–174.

[8] C. Kurehong, C. Kanchanawarin, B. Powthongchin, G. Katzenmeier, C. Angsuthanasombat, Membrane-pore forming characteristics of the Bordetella pertussis CyaA-hemolysin domain, Toxins 7 (2015) 1486–1496.

[9] B. Powthongchin, C. Angsuthanasombat, Effects on haemolytic activity of single proline substitutions in the *Bordetella pertussis* CyaA pore-forming fragment, Arch. Microbiol. 191 (2009) 1–9.

[10] S. Juntapremjit, N. Thamwiriyasati, C. Kurehong, P. Prangkio, L. Shank, B. Powthongchin, C. Angsuthanasombat, Functional importance of the Gly cluster in transmembrane helix 2 of the *Bordetella pertussis* CyaA-hemolysin: implications for toxin oligomerization and pore formation, Toxicon 106 (2015) 14–19.

[11] C. Kurehong, C. Kanchanawarin, B. Powthongchin, P. Prangkio, G. Katzenmeier, C. Angsuthanasombat, Functional contributions of positive charges in the pore-lining helix 3 of the *Bordetella pertussis* CyaA-hemolysin to hemolytic cctivity and ion-channel opening, Toxins 9 (2017) 109–121.

[12] P. Prangkio, S. Juntapremjit, M. Koehler, P. Hinterdorfer, C. Angsuthanasombat, Contributions of the hydrophobic helix 2 of the *Bordetella pertussis* CyaA-hemolysin to membrane permeabilization, Protein Pept. Lett. 25 (2018) 1–8.

[13] M. Hackett, L. Guo, J. Shabanowitz, D.F. Hunt, E.L. Hewlett, Internal lysine palmitoylation in adenylate cyclase toxin from *Bordetella pertussis*, Science 266 (1994) 433–435.

[14] T. Basar, V. Havlicek, S. Bezouskova, M. Hackett, P. Sebo, Acylation of lysine 983 is sufficient for toxin activity of *Bordetella pertussis* adenylate cyclase; substitutions of alanine 140 modulate acylation site selectivity of the toxin acyltransferase CyaC, J. Biol. Chem. 276 (2001) 348–354.

[15] C. Bauche, A. Chenal, O. Knapp, C. Bodenreider, R. Benz, A. Chaffotte, D. Ladant, Structural and functional characterization of an essential RTX subdomain of *Bordetella pertussis* adenylate cyclase toxin, J. Biol. Chem. 281 (2006) 16914–16926.

[16] T. Rose, P. Sebo, J. Bellalou, D. Ladant, Interaction of calcium with *Bordetella pertussis* adenylate cyclase toxin, J. Biol. Chem. 270 (1995) 26370–26376.

[17] I. Linhartova, L. Bumba, J. Masin, M. Basler, R. Osicka, J. Kamanova, K. Prochazkova, I. Adkins, J. Hejnova-Holubova, L. Sadilkova, J. Morova, P. Sebo, RTX proteins: a highly diverse family secreted by a common mechanism, FEMS Microbiol. Rev. 34 (2010) 1076–1112.

[18] P. Pojanapotha, N. Thamwiriyasati, B. Powthongchin, G. Katzenmeier, C. Angsuthanasombat, *Bordetella pertussis* CyaA-RTX subdomain requires calcium ions for structural stability against proteolytic degradation, Protein Expr. Purif. 75 (2011) 127–132.

[19] L. Bumba, J. Masin, P. Macek, T. Wald, L. Motlova, I. Bibova, N. Klimova, L. Bednarova, V. Veverka, M. Kachala, Dmitri I. Svergun, C. Barinka, P. Sebo, Calcium-driven folding of RTX domain β-rolls ratchets translocation of RTX proteins through type I secretion ducts, Mol. Cell 62 (2016) 47–62.

[20] J.C. Karst, V.Y. Ntsogo Enguene, S.E. Cannella, O. Subrini, A. Hessel, S. Debard, D. Ladant, A. Chenal, Calcium, acylation, and molecular confinement favor folding of *Bordetella pertussis* adenylate cyclase CyaA toxin into a monomeric and cytotoxic, J. Biol. Chem. 289 (2014) 30702–30716.

[21] J. Masin, M. Basler, O. Knapp, M. El-Azami-El-Idrissi, E. Maier, I. Konopasek, R. Benz, C. Leclerc, P. Sebo, Acylation of lysine 860 allows tight binding and cytotoxicity of *Bordetella* adenylate cyclase on CD11b-expressing cells, Biochemistry 44 (2005) 12759–12766.

[22] K. Meetum, C. Imtong, G. Katzenmeier, C. Angsuthanasombat, Acylation of the *Bordetella pertussis* CyaA-hemolysin: functional implications for efficient membrane insertion and pore formation, Biochim. Biophys. Acta Biomembr. 1859 (2017) 312–318.

[23] R.A. Pandit, K. Meetum, K. Suvarnapunya, G. Katzenmeier, W. Chaicumpa, C. Angsuthanasombat, Isolated CyaA-RTX subdomain from *Bordetella pertussis*: structural and functional implications for its interaction with target erythrocyte membranes, Biochem. Biophys. Res. Commun. 466 (2015) 76–81.

[24] V. Raksanoh, L. Shank, P. Prangkio, M. Yentongchai, S. Sakdee, C. Imtong, C. Angsuthanasombat, Zn^{2+}-dependent autocatalytic activity of the *Bordetella pertussis* CyaA-hemolysin, Biochem. Biophys. Res. Commun. 485 (2017) 720–724.

[25] N. Thamwiriyasati, B. Powthongchin, J. Kittiworakarn, G. Katzenmeier, C. Angsuthanasombat, Esterase activity of *Bordetella pertussis* CyaC-acyltransferase against synthetic substrates: implications for catalytic mechanism *in vivo*, FEMS Microbiol. Lett. 304 (2010) 183–190.

[26] W. Sriwimol, A. Aroonkesorn, S. Sakdee, C. Kanchanawarin, T. Uchihashi, T. Ando, C. Angsuthanasombat, Potential pre-pore trimer formation by the *Bacillus thuringiensis* mosquito-specific toxin: molecular insights into a critical prerequisite of membrane-bound monomers, J. Biol. Chem. 290 (2015) 20793–20803.

[27] N.P. Greene, A. Crow, C. Hughes, V. Koronakis, Structure of a bacterial toxin-activating acyltransferase, Proc. Nat. Acad. Sci. USA 112 (2015) 3058–3066.

[28] C. Kurehong, B. Powthongchin, N. Thamwiriyasati, C. Angsuthanasombat, Functional significance of the highly conserved Glu^{570} in the putative pore-forming helix 3 of the *Bordetella pertussis* haemolysin toxin, Toxicon 57 (2011) 897–903.

[29] J. Li, P.C. Edwards, M. Burghammer, C. Villa, G.F. Schertler, Structure of bovine rhodopsin in a trigonal crystal form, J. Mol. Biol. 343 (2004) 1409–1438.

[30] S. Bienert, A. Waterhouse, Tjaart A.P. de Beer, G. Tauriello, G. Studer, L. Bordoli, T. Schwede, The SWISS-MODEL Repository—new features and functionality, Nucleic Acids Res. 45 (2017) D313–D319.

[31] P. Benkert, M. Biasini, T. Schwede, Toward the estimation of the absolute quality of individual protein structure models, Bioinformatics 27 (2011) 343–350.

[32] N.A. Baker, D. Sept, S. Joseph, M.J. Holst, J.A. McCammon, Electrostatics of nanosystems: application to microtubules and the ribosome, Proc. Natl. Acad. Sci. U.S.A. 98 (2001) 10037–10041.

[33] D. Kozakov, D.R. Hall, B. Xia, K.A. Porter, D. Padhorny, C. Yueh, D. Beglov, S. Vajda, The ClusPro web server for protein–protein docking, Nat. Protoc. 12 (2017) 255–278.